DEUTSCHES ELEKTRONEN-SYNCHROTRON

DESY 96–230
November 1996

Energy Fluctuation Analysis in Integrable Billiards in Hyperbolic Geometry

C. Grosche

II. Institut für Theoretische Physik, Universität Hamburg

and

Institut für Theoretische Physik, Technische Universität Clausthal, Clausthal-Zellerfeld

ISSN 0418-9833

NOTKESTRASSE 85 - 22607 HAMBURG

To be sure that your preprints are promptly included in the
HIGH ENERGY PHYSICS INDEX,
send them to (if possible by air mail):

DESY	**DESY-IfH**
Bibliothek	**Bibliothek**
Notkestraße 85	**Platanenallee 6**
22603 Hamburg	**15738 Zeuthen**
Germany	**Germany**

DESY 96–230 ISSN 0418 - 9833
November 1996

ENERGY FLUCTUATION ANALYSIS IN INTEGRABLE BILLIARDS IN HYPERBOLIC GEOMETRY

Ch. Grosche

II. Institut für Theoretische Physik
Universität Hamburg, Luruper Chaussee 149
22761 Hamburg, Germany
and
Institut für Theoretische Physik
Technische Universität Clausthal, Sommerfeldstraße 6
38678 Clausthal-Zellerfeld, Germany

ABSTRACT

In this contribution I provide new examples of integrable billiard systems in hyperbolic geometry. In particular, I present one billiard system in the hyperbolic plane, called "Circular billiard in the Poincaré disc", and one three-dimensional billiard, called "Spherical billiard in the Poincaré ball". In each of the billiard systems, the quantization condition leads to transcendental equations for the energy eigen-values E_n, which must be solved numerically. The energy eigen-values are statistically analysed with respect to spectral rigidity and the normalized fluctuations about Weyl's law. For comparison, some flat two- and three-dimensional billiard systems are also mentioned. The found results are in accordance with the semiclassical theory of the spectral rigidity of Berry, and the conjecture of Steiner et al. concerning the normalized fluctuations for integrable billiard systems.

1 Introduction.

Billiard systems have become recently more and more popular. The particle is allowed to move freely within the boundaries of the billiard and no potential term is taken into account. Of particular interest have been the investigations of the statistical analysis of the energy spectra. Due to Berry [8] is a classification into at least two universality classes: The first universality class occurs for classically integrable systems. Here the spectral rigidity $\Delta_3(L)$ of Dyson and Metha [15] is according to $\Delta_3(L) \simeq L/15$ in the range $0 \leq L < L_M$, with $L_M = \sqrt{\pi\mathcal{E}_M}$ a maximal value. For $L > L_M$, $\Delta_3(L)$ approaches a saturation value Δ_∞ which grows according to $\Delta_\infty = c_{\Delta_\infty}\sqrt{\mathcal{E}}$, where c_{Δ_∞} a characteristic constant of the system.

The second universality class occurs for (generic) classically chaotic systems, and in these systems $\Delta_3(L)$ increases logarithmically for $0 \leq L < L_M$; for $L > L_M$, $\Delta_3(L)$ approaches again a saturation value Δ_∞ which grows according to $\Delta_\infty = c_{\Delta_\infty}\ln\mathcal{E}$, and c_{Δ_∞} is again a characteristic constant of the billiard system.

If the systems are analysed with respect to, e.g., nearest neighbour statistics, one finds for desymmetrized classical integrable systems a Poisson distribution, and for classically chaotic systems either a GOE or a GUE distribution, depending whether time-reversal invariance is valid or not. Another tool is the number variance $\Sigma_2(L)$, where one has in average $\Sigma_2(L) \simeq 2\Delta_3(L)$, as $L \to \infty$. More interesting is the *distribution* of the fluctuations of the spectral staircase of a system about Weyl's law. This distribution seems to be a principal tool to distinguish on the quantal level whether the corresponding classical system is integrable or chaotic. By "classically chaotic" I mean in the following a system which has less conserved quantities, energy, (angular) momentum etc., as its dimensionality is. For instance, a conservative one-dimensional systems is always integrable, the conserved quantity being the energy. For two-dimensional systems the feature changes, because we can either have two conserved quantities, i.e., the energy and a "momentum", or only one conserved quantity, i.e., the energy. The latter system, or course, is called "classically chaotic". In three dimensions the feature gets more complicated, because we can have one, two or three conserved quantities. The first is chaotic, the third is integrable, and the second has some sort of mixed properties, e.g., the diamagnetic Kepler problem [22].

Steiner et al. [1, 34] have formulated a conjecture and have claimed that it can be justified that the typical feature of quantum chaos has been found. They have argued that there are unique fluctuation properties in quantum mechanics which are universal and maximally random if the corresponding classical system is strongly chaotic. For this, one determines first the fluctuations of the spectral staircase about Weyl's law $\delta_n := n - 1/2 - \bar{N}(E_n)$. Second, the normalized fluctuations $\alpha_n = \delta_n/a_n(E)$ are considered, where $a_n(E) = \sqrt{c_{\Delta_\infty}\sqrt{\mathcal{E}}}$ for two-dimensional classically integrable systems, and $a_n(E) = \sqrt{c_{\Delta_\infty}\ln\mathcal{E}}$ for (generic) classically chaotic systems. The conjecture states that for strongly chaotic systems the distribution $P(\alpha_n)$ of the normalized fluctuations α_n, considered as random numbers, have due to the central limit theorem a limit distribution $P(\alpha)$, which is Gaussian with mean zero and standard deviation one. Steiner et al. gave evidence for their conjecture in the examples of a generic hyperbolic octagon [1, 34], hyperbolic triangles [1, 3, 34], Artin's billiard [34], the hyperbola billiard [1, 31], and the cardioid billiard [5]. Their studies are based on the Selberg trace formula [25, 30] and the semiclassical Gutzwiller-Sieber-Steiner (GSS) trace formula for non-integrable systems [22, 31, 33], which connects the quantal energy-eigenvalues with the lengths of the unstable isolated periodic classical orbits.

However, in contrast to the universal situation for chaotic systems, the situation is quite different for classically integrable systems. Whereas it follows from the spectral rigidity [1, 11] that the normalized fluctuations for classically integrable systems still give a distribution with mean zero and deviation one, there seems to be in general no central limit theorem for the fluctuations, and the profile of the density $P(\alpha)$ can be very different for different systems. Indeed, in a particular integrable billiard system in the hyperbolic strip, called "Hyperbolic rectangle in the hyperbolic strip" [18], I have found for the distribution of the normalized fluctuations that they are non-Gaussian with skewness $\kappa \neq 0$ [21], therefore displaying the expected features of the conjecture for classically integrable systems. In fact, for certain systems it can be explicitly proven that the limit distribution is definitely non-Gaussian, e.g., for the circle [10] or for the square, respectively rectangles [24, 28] with a behaviour according to $P(\alpha) \propto c_1 e^{-c_2\alpha^4}$, or the so-called Zoll-surfaces [29] with a limit distribution $P(\alpha) \propto 1/b$ in the interval $|\alpha| < b/2$. For classically integrable systems the analogue of the GSS-formula is the trace formula of Berry and Tabor [9].

Whereas the original motivation for the study of such a system was to search for remainders of the chaotic system in a classical integrable system and to demonstrate the semiclassical theory of spectral rigidity of Berry [8], integrable billiard system in spaces of non-constant curvature also serve as test-models for the conjecture of Steiner et al. In this contribution I present two more integrable systems in hyperbolic geometry: First, as a two-dimensional system, the circle billiard in the Poincaré disc, and as a three-dimensional system, the sphere billiard in the Poincaré ball. In addition, I also mention the hyperbolic triangle, i.e., the truncated modular domain, as introduced by Graham et al. [14] from this point of view. For completeness I list also some flat two- and three-dimensional billiard systems in order to give a comprehensive look at some important features for various billiard systems in two and three dimensions. These systems are flat rectangles and flat parallelepipeds with irrational ratios of sides, respectively.

In the sequel I present shortly in the next section the required techniques for the numerical analysis for billiard systems, i.e., Weyl's law in two and three dimensions, the definition of the number variance Σ_2 and the spectral rigidity Δ_3. In the third section I present the two new models, which includes the statement of the quantization conditions, the number variance and spectral rigidity, and the distribution $P(\alpha_n)$. For completeness also the results of the hyperbolic rectangles and a hyperbolic triangle are included. The fourth section contains the numerical results, and the fifth a summary.

2 Weyl's Law and Spectral Rigidity.

2.1 Weyl's Law.

Weyl's law describes the increase of modes in a two- or three-dimensional cavity with increasing energy. Normally, one can take into account Dirichlet and Neumann boundary conditions, where it is possible to assign to each "wall" independently one of the two boundary conditions. Assuming Dirichlet or Neumann boundary conditions selects wave-functions with odd and even parity with respect to reflection to a symmetry axis. Mathematically, the time-independent Schrödinger equation turns out to be a stationary wave-equation, and the quantum problem is formally equivalent to a electrodynamical cavity problem. For Dirichlet boundary conditions Weyl's law in two dimensions has the

form, e.g. [7],

$$N(E) = \frac{AE}{4\pi} - \frac{\partial A}{4\pi}\sqrt{E} + \frac{1}{24}\sum_{corners}\left(\frac{\pi}{\alpha_r} - \frac{\alpha_r}{\pi}\right) + \frac{1}{12\pi}\iint_A K(\sigma)d\sigma - \frac{1}{24\pi}\oint_{\partial A}\kappa(s)ds + O\left(\frac{1}{\sqrt{E}}\right) . \qquad (2.1)$$

Here α_r denotes the angle of the r^{th}-corner, A the area of the system, and ∂A the length of its boundary. K is the Gaussian curvature, $d\sigma$ the surface integral, and κ the boundary mean curvature.

In three dimensions Weyl's law is given by [2, 6, 7]

$$N(E) = A\,E^{3/2} + B\,E + C\,E^{1/2} + D \ , \qquad (2.2)$$

with the constants A, B, C, D given by (smooth boundaries and Dirichlet boundary conditions required)

$$\left.\begin{aligned} A &= \frac{\text{Volume}}{6\pi^2} \ , \qquad B = -\frac{\text{Area}}{16\pi} \ , \\ C &= \frac{1}{12\pi^2}\int_{\partial A} d\sigma\left(\frac{1}{R_1} + \frac{1}{R_2}\right) \ , \\ D &= \frac{1}{512\pi^2}\int_{\partial A} d\sigma\left(\frac{1}{R_1} - \frac{1}{R_2}\right)^2 \ ; \end{aligned}\right\} \qquad (2.3)$$

where R_1, R_2 are the two main curvature radii at each point of the boundary. In the case of a volume with polyhedral domains and polygonal crossections, C and D are given by [7]

$$C = \frac{1}{12\pi}\sum_j\left(\frac{\pi}{\alpha_j} - \frac{\alpha_j}{\pi}\right)L_j \ , \qquad D = -\frac{1}{48}\sum_j\left(\frac{\pi}{\alpha_j} - \frac{\alpha_j}{\pi}\right) \ , \qquad (2.4)$$

where L_j denotes the length of the jth edge.

2.2 Statistical Analysis.

A first analysis gives the level-spacing distribution $P(S)$ of spacings between neighbouring levels. Classically integrable systems belong to the universality class of uncorrelated level sequences. $P(S)$ is calculated for the scaled energy spectrum, which has a mean level spacing of one ($= \hbar$). One applies Weyl's law onto the calculated energy levels and obtains the normalized levels $\mathcal{E}_n$ by $\mathcal{E}_n = N(E_n)$, and quantities for the scaled spectrum are denoted by $\mathcal{E}$ in the following. In integrable systems one typically has level clustering, which is expressed by $P(S) \to 1$, as $S \to 0$, whereas chaotic systems show level repulsion, i.e. $P(S) \to 0$ as $S \to 0$. The functional form of the nearest neighbour level spacing $P(S)$ for classically integrable systems has the form

$$P(S) = e^{-S} \ , \qquad (2.5)$$

which is a Poisson distribution. The result from random matrix theory for the level spacing distribution of a GOE-ensemble is approximated by a Wigner distribution

$$P(S) = \frac{\pi}{2}S\,e^{-\pi S^2/4} \ , \qquad (2.6)$$

and the corresponding level spacing distribution of a GUE-ensemble is given by

$$P(S) = \frac{32}{\pi^2}S^2 e^{-4S^2/\pi} \ . \qquad (2.7)$$

The level spacing distribution $P(S)$ is a short range statistics. Another important tool in the analysis of the spectrum is the number variance $\Sigma_2(L)$ and the spectral rigidity $\Delta_3(L)$ of Metha and Dyson [15], respectively. $\Sigma_2(L)$ is defined as the local variance of the number $n(\mathcal{E}, L)$ of scaled energy levels in the interval from $\mathcal{E} - L/2$ to $\mathcal{E} + L/2$. It is defined as

$$\Sigma_2(L) = \left\langle n(\mathcal{E}, L) - L^2 \right\rangle \ . \tag{2.8}$$

The Δ_3 statistics is defined as the local average of the mean square deviation of the staircase $N'(\mathcal{E})$ from the best fitting of a straight line over an energy range corresponding to L mean level spacings, namely

$$\Delta_3(L) = \left\langle \min_{(a,b)} \frac{1}{L} \int_{-L/2}^{L/2} d\epsilon [N'(\mathcal{E} + \epsilon) - a - b\epsilon]^2 \right\rangle \ . \tag{2.9}$$

It can be expressed as

$$\Delta_3(L) = \left\langle \frac{1}{L} \int\limits_{-L/2}^{L/2} d\epsilon N'^2(\mathcal{E} + \epsilon) - \left[\frac{1}{L} \int\limits_{-L/2}^{L/2} d\epsilon N'(\mathcal{E} + \epsilon) \right]^2 - 12 \left[\frac{1}{L^2} \int\limits_{-L/2}^{L/2} d\epsilon N'(\mathcal{E} + \epsilon) \right]^2 \right\rangle \ . \tag{2.10}$$

As the number variance, it characterizes long-term correlations of the energy levels. Both statistics are related by

$$\Delta_3(L) = \frac{2}{L_4} \int_0^L ds (L^3 - 2L^2 s - s^3) \Sigma_2(s) \ . \tag{2.11}$$

Whenever $L \ll 1$, the very fact that $N(E)$ is a staircase leads in this limit to [8]

$$\Sigma_2(S) = L \ , \qquad \Delta_3(L) = \frac{L}{15} \ , \tag{2.12}$$

and both statistics are linear and show the so-called Poissonian behaviour, i.e. in the case of a genuine Poisson distributed level sequence, these results are exact. The spectral rigidity gives therefore no information about the very finest scales corresponding to the spacings between neighbouring levels, whether they are Poisson distributed or not. Its usefulness lies in the way it describes level sequences larger than the inner energy scale ($L = 1$) of a system. Berry [8] has developed a semiclassical theory of the spectral rigidity and has shown that one must discriminate between at least two universality classes of rigidity, depending on whether one deals with classically integrable systems or classically chaotic systems. The first universality class occurs for classically integrable systems. Here the Poisson $L/15$-form for the spectral rigidity extends from $L = 0$ to L_{Max}. L_{Max} corresponds to an outer energy scale $\propto 1/T_{Min}$ (the inner energy scale corresponds to $L \simeq 1$), where T_{Min} is the period of the shortest classical orbit and $L_{Max} \propto \hbar^{N-1}$, and $\propto 1/\hbar$ for $N = 2$ (i.e. a two-dimensional system). The properties of the rigidity are determined by the contributions of the very short orbits. These orbits have a non-universal behaviour, which differ from system to system. As a consequence of the fact that there is a shortest orbit, the spectral rigidity saturates and approaches a non-universal constant Δ_∞, as $L \to \infty$ (and the same line of reasoning is true for the number variance Σ_2) [4, 8, 31]. The number variance for a GOE-distributed sequences is given by [12, 15, 23]

$$\Sigma_2(L) = \frac{2}{\pi^2} \Big\{ \log(2\pi L) + \gamma + 1 + \frac{1}{2}\mathrm{Si}^2(\pi L) - \frac{\pi}{2}\mathrm{Si}(\pi L) - \cos(2\pi L) - \mathrm{Ci}(2\pi L) + \pi^2 L \Big[1 - \frac{2}{\pi}\mathrm{Si}(2\pi L) \Big] \Big\} \ , \tag{2.13}$$

and for GUE-distributed sequences [4, 12, 23, 31], respectively,

$$\Sigma_2(L) = \frac{1}{\pi^2} \Big\{ \log(2\pi L) + \gamma + 1 - \cos(2\pi L) - \mathrm{Ci}(2\pi L) + \pi^2 L \Big[1 - \frac{2}{\pi}\mathrm{Si}(2\pi L) \Big] \Big\} \ . \tag{2.14}$$

Results for the spectral rigidity are obtained via the relation (2.11).

3 The Models and Their Quantization Conditions.

I now give a short overview of some known billiard systems, as well as the billiards in hyperbolic geometry.

3.1 Flat Billiards

3.1.1 The square.

The simplest systems are *rectangular billiards* in flat space (Euclidean rectangles) [13], where the energy levels are simply given by

$$E_{n_1,n_2} = \pi^2 \left(\frac{n_1^2}{a^2} + \frac{n_2^2}{b^2} \right) \ , \tag{3.1}$$

with n_1, n_2 natural numbers and a, b the sides of the rectangle, and I have taken natural units $\hbar = 2m = 1$. Weyl's law has the form [7]

$$\bar{N}(E) \simeq \frac{ab}{4\pi} E - \frac{a+b}{2\pi} \sqrt{E} + \frac{1}{4} \ . \tag{3.2}$$

Usually one uses $a = 1$, with b varying. It can be proven that the limit distribution $P(\alpha)$ is non-Gaussian [24, 28]. The system has been investigated by Casati et al. [13] and by Berry [8].

3.1.2 The sphere.

The second system in flat space is the *circular billiard* with radius R and area $A = \pi R^2$. The energy levels are given by

$$E_{l,n} = j_{l,n}^2 / R^2 \ , \qquad l = 0, 1, \ldots, \qquad n = 1, 2, \ldots, \tag{3.3}$$

where $x_n = j_{l,m}$ is the n-th zero of the Bessel function $J_l(x)$. Weyl's law has the form [7]

$$\bar{N}(E) \simeq \frac{R^2}{4} E - \frac{R}{2} \sqrt{E} + \frac{1}{6} \ . \tag{3.4}$$

The circle billiard has been studied by, e.g., Kim [27] it has been shown that the distribution of the energy fluctuations is non-Gaussian and skew.

3.1.3 The parallelepiped.

The simplest three-dimensional system is a *rectangular parallelepiped* with sides a, b, c in flat space, where the energy levels are simply given by

$$E_{n_1,n_2} = \pi^2 \left(\frac{n_1^2}{a^2} + \frac{n_2^2}{b^2} + \frac{n_3^2}{c^2} \right) \ , \tag{3.5}$$

with n_1, n_2, n_3 natural numbers. Weyl's law has the form [7]

$$N(E) \simeq \frac{abc}{6\pi^2}E^{3/2} - \frac{ab+bc+ac}{8\pi}E + \frac{a+b+c}{2\pi}\sqrt{E} - \frac{1}{8} \ . \tag{3.6}$$

3.2 Hyperbolic Billiards

3.2.1 The hyperbolic rectangle.

The *hyperbolic rectangle* [18] is defined by a rectangular domain in the hyperbolic strip $S = \{(X,Y)|X \in \mathbb{R}, |Y| < \pi/2\}$ endowed with the corresponding hyperbolic geometry $ds^2 = (dX^2 + dY^2)/\cos^2 Y$ [17, 21]. Even and odd parity with respect to the X-coordinate yields the quantization condition with respect to the X-dependence

$$\text{even:} \quad k_l = \frac{2\pi(l+1/2)}{L_0} \ , \quad l = 0,1,2,\dots \ , \qquad \text{odd:} \quad k_l = \frac{2\pi l}{L_0} \ , \quad l = 1,2,3,\dots \ . \tag{3.7}$$

$2L_0$ denotes the width of the rectangle in the coordinate X, assuming Dirichlet boundary conditions at $X = \pm L_0$. Even and odd parity with respect to the Y-coordinate then gives the quantization conditions

$$\text{even/odd:} \qquad P^{ip_n}_{ik_l-1/2}(\sin Y_0) \pm P^{ip_n}_{ik_l-1/2}(-\sin Y_0) = 0 \ . \tag{3.8}$$

$2Y_0$ denotes the width of the rectangle in the coordinate Y, assuming Dirichlet boundary conditions at $Y = \pm Y_0$. The last two equations are transcendental equations for p_n, $n = 1,2,\dots$, and must be solved numerically yielding the energy levels $E_n = p_n^2 + 1/4$. The above quantization rule follows from the path integral representation incorporating boundary conditions at $X = \pm L_0, Y = \pm Y_0$ according to [20]

$$\begin{aligned}
&G_{(|Y|<Y_0,|X|<L_0)}(X'',X',Y'',Y';E)\\
&= \frac{i}{\hbar}\int_0^\infty dT\, e^{iET/\hbar} \int\limits_{X(t')=X'}^{X(t'')=X''} \mathcal{D}_{(|X|<L_0)}X(t) \int\limits_{Y(t')=Y'}^{Y(t'')=Y''} \mathcal{D}_{(|Y|<Y_0)}Y(t) \exp\left(\frac{im}{2\hbar}\int_{t'}^{t''}\frac{\dot X^2 + \dot Y^2}{\cos^2 Y}dt\right)\\
&= \frac{2\pi}{L_0}\sum_{l=0}^\infty \begin{pmatrix} \sin(k_l X')\sin(k_l X'') \\ \cos(k_l X')\cos(k_l X'') \end{pmatrix}\\
&\quad \times \frac{\begin{vmatrix} G_0(Y'',Y';E) & G_0(Y'',-Y_0;E) & G_0(Y'',Y_0;E) \\ G_0(-Y_0,Y';E) & G_0(-Y_0,-Y_0;E) & G_0(-Y_0,Y_0;E) \\ G_0(Y_0,Y';E) & G_0(Y_0,-Y_0;E) & G_0(Y_0,Y_0;E) \end{vmatrix}}{\begin{vmatrix} G_0(-Y_0,-Y_0;E) & G_0(-Y_0,Y_0;E) \\ G_0(Y_0,-Y_0;E) & G_0(Y_0,Y_0;E) \end{vmatrix}} \ ,
\end{aligned} \tag{3.9}$$

with k_l chosen accordingly for odd/even states in X, and $G_0(E)$ for the unrestricted motion in Y is given by [26]

$$\begin{aligned}
G_0(Y'',Y';E) = \frac{m}{\hbar^2}\Gamma\Big(\frac{1}{\hbar}\sqrt{-2mE} - ik_l + \frac{1}{2}\Big)\Gamma\Big(\frac{1}{\hbar}\sqrt{-2mE} + ik_l + \frac{1}{2}\Big)\\
\times P^{-\sqrt{-2mE}/\hbar}_{ik_l-1/2}(\sin Y_>)P^{-\sqrt{-2mE}/\hbar}_{ik_l-1/2}(-\sin Y_<) \ .
\end{aligned} \tag{3.10}$$

For the entire hyperbolic rectangle Weyl's law has the form

$$N(E) \simeq E - \frac{\sqrt{E}}{4\pi}\left[4\ln\left(\frac{1+\sin Y_0}{\cos Y_0}\right) + \frac{2L_0}{\cos Y_0}\right] - \frac{1}{12} + \frac{L_0\tan Y_0}{48\cos^2 Y_0} \ , \tag{3.11}$$

and similarly for the desymmetrized domains, where one takes into account Dirichlet and Neumann boundary conditions on the lines $X = 0$ and $Y = 0$, respectively. L_0 and Y_0 are chosen in such a way that the area of the entire rectangle is 4π [18]. For the numerical investigation one uses the representation [16, p.1009]

$$P^{ip}_{ik-\frac{1}{2}}(\sin Y) = \frac{1}{\Gamma(1-ip)}\left(\frac{1+\sin Y}{1-\sin Y}\right)^{ip/2} {}_2F_1\Big(\frac{1}{2} - ik, \frac{1}{2} + ik; 1 - ip; \frac{1-\sin Y}{2}\Big) \ , \tag{3.12}$$

and omits the $1/\Gamma(1-ip)$-factor. This system has been investigated in [18, 21] and it has been given evidence that the limit distribution is non-Gaussian and skew.

3.2.2 The hyperbolic circle.

The *hyperbolic circle* is defined as a circle in the Poincaré disc $D = \{(r,\varphi)|r < 1, \varphi \in [0,2\pi)\}$ endowed with the corresponding hyperbolic geometry $ds^2 = (dr^2 + r^2 d\varphi^2)/(1-r^2)^2$ [17, 21]. Choosing $r = 1/\sqrt{2}$ yields $A = 4\pi$, and the quantization condition is given by the transcendental equation (assuming Dirichlet boundary conditions at $r = 1/\sqrt{2}$, i.e., $\cosh R = 3$, and $R = \text{arcosh}3 = 1.762,747,174,\dots$)

$$\mathcal{P}^{-l}_{-1/2+ip_n}(3) = 0 \ , \qquad l = 0,1,\dots, \qquad n = 1,2\dots \ , \tag{3.13}$$

where $\mathcal{P}^\mu_\nu(z)$ are Legendre functions. The quantization condition follows from considering the path integral representation of the two-dimensional hyperboloid in the domain $\tau < R$ which in (pseudo-) spherical coordinates has the form

$$\begin{aligned}
K(\tau'',\tau',\varphi'',\varphi';T) &= \int\limits_{\tau(t')=\tau'}^{\tau(t'')=\tau''} \mathcal{D}_{(\tau<R)}\tau(t)\sinh\tau \int\limits_{\varphi(t')=\varphi'}^{\varphi(t'')=\varphi''} \mathcal{D}\varphi(t)\\
&\quad\times\exp\left\{\frac{i}{\hbar}\int_{t'}^{t''}\left[\frac{m}{2}(\dot\tau^2 + \sinh^2\tau\dot\varphi^2) - \frac{\hbar^2}{8m}\Big(1 - \frac{1}{\sinh^2\tau}\Big)\right]dt\right\}\\
&= (\sinh\tau'\sinh\tau'')^{-1/2}\sum_{\nu\in\mathbb{Z}}\frac{e^{i\nu(\varphi''-\varphi')}}{2\pi}\\
&\quad\times\int\limits_{\tau(t')=\tau'}^{\tau(t'')=\tau''} \mathcal{D}_{(\tau<R)}\tau(t)\exp\left\{\frac{i}{\hbar}\int_{t'}^{t''}\left[\frac{m}{2}\dot\tau^2 - \frac{\hbar^2}{2m}\frac{\nu^2 - 1/4}{\sinh^2\tau}\right]dt\right\} \ .
\end{aligned} \tag{3.14}$$

The remaining τ-path integration gives for the free (unrestricted) motion for the corresponding Green function ($E = \frac{\hbar^2}{2m}(p_E^2 + 1/4)$)

$$G_\nu(\tau'',\tau';E) = \frac{2m}{\hbar^2}\sqrt{\sinh\tau'\sinh\tau''}\, e^{-i\pi\nu}\mathcal{P}^{-\nu}_{-1/2+ip_E}(\cosh\tau_<)\mathcal{Q}^\nu_{-1/2+ip_E}(\cosh\tau_>) \ , \tag{3.15}$$

where $\tau_{<,>}$ denotes the smaller, respectively larger of τ', τ''. Denoting by $A(\tau) = \mathcal{Q}_{-1/2+ip_E}(\cosh\tau)$, $B(\tau) = \mathcal{P}_{-1/2+ip_E}(\cosh\tau)$, we obtain according to [19, 20] the Green function $G_{(\nu,\tau<R)}(E)$ for the restricted system with $\tau < R$

$$G_{(\nu,\tau<R)}(\tau'',\tau';E) = \frac{2m}{\hbar^2}e^{-i\pi\nu}\sqrt{\sinh\tau'\sinh\tau''}\left\{A_E(\tau_>)B_E(\tau_<) - \frac{A_E(R)}{B_E(R)}B_E(\tau')B_E(\tau'')\right\} \ . \tag{3.16}$$

For $\nu \geq 1$ the energy levels $E_n = p_n^2 + 1/4$ are two-fold degenerate, and Weyl's law has the form

$$\bar{N}(E) \simeq E - \sqrt{2E} + \frac{\sqrt{2}-1}{3} \ . \tag{3.17}$$

For the numerical investigation of the zeros of the transcendental equation (3.13) one uses the representation [16, p.1010]

$$\begin{aligned}\mathcal{P}_\nu^\mu(z) &= \frac{\Gamma(-\nu-1/2)}{2^{\nu+1}\sqrt{\pi}\,\Gamma(-\nu-\mu)}(z^2-1)^{-(\nu+1)/2}{}_2F_1\Big(\frac{\nu-\mu+1}{2},\frac{\nu+\mu+1}{2};\nu+\frac{3}{2};\frac{1}{1-z^2}\Big)\\ &\quad \frac{2^\nu\Gamma(\nu+1/2)}{\sqrt{\pi}\,\Gamma(\nu-\mu+1)}(z^2-1)^{\nu/2}{}_2F_1\Big(\frac{\mu-\nu}{2},\frac{\nu-\mu}{2};\frac{1}{2}-\nu;\frac{1}{1-z^2}\Big) \ ,\end{aligned} \tag{3.18}$$

and in addition to avoid numerical overflow effects the multiplication formula of the Γ-function [16, p.937]

$$\Gamma(nz) = (2\pi)^{(1-n)/2} n^{nz-1/2} \prod_{k=0}^{n-1} \Gamma\Big(z+\frac{k}{n}\Big) \ . \tag{3.19}$$

3.2.3 The hyperbolic triangle.

The last two-dimensional system in hyperbolic geometry is a *hyperbolic triangle* [14] in the Poincaré upper half-plane $\mathcal{H} = \{(x,y)|y>0, x\in\mathbb{R}\}$, endowed with the corresponding geometry $ds^2 = (dx^2+dy^2)/y^2$ [17, 21], defined by $y>1, |x|<1/2$ [14]. The hyperbolic triangle is a non-compact domain with area $A = 1/2$. The energy levels $E_n = p_n^2 + 1/4$ are implicitly defined by

$$K_{\mathrm{i}p_n}(l\pi) \ , \qquad l = 2,4,\dots, \qquad n = 1,2,\dots, \tag{3.20}$$

where $K_\nu(x)$ is a modified Bessel function. Weyl's law has the form (assuming Dirichlet boundary conditions at $y=1$ and $x=\pm 1/2$) [14]

$$\bar{N}(E) \simeq \frac{E}{8\pi} - \frac{\ln E\sqrt{E}}{4\pi} + \frac{3/2 - 2\ln 2}{4\pi}\sqrt{E} + \frac{\pi}{2} \ . \tag{3.21}$$

The $\ln E\sqrt{E}$-term is typically for non-compact billiards. The quantization condition can be derived form the path integral representation [14, 21]

$$\begin{aligned}K(y'',y',x'',x';T) &= \int\limits_{y(t')=y'}^{y(t'')=y''} \frac{\mathcal{D}_{(y>1)}y(t)}{y^2} \int\limits_{x(t')=x'}^{x(t'')=x''} \mathcal{D}x(t) \exp\Big(\frac{\mathrm{i}m}{2\hbar}\int_{t'}^{t''}\frac{\dot{y}^2+\dot{x}^2}{y^2}dt\Big)\\ &= \sqrt{y'y''}\sum_{l=1,3,\dots}\sin\big[l\pi(x-\tfrac{1}{2})\big]\\ &\quad\times \int\limits_{y(t')=y'}^{y(t'')=y''} \frac{\mathcal{D}_{(y>1)}y(t)}{y} \exp\Big[\frac{\mathrm{i}}{\hbar}\int_{t'}^{t''}\Big(\frac{\dot{y}^2}{y^2} - \frac{\hbar^2 l^2\pi^2}{2my^2}\Big)dt - \frac{\mathrm{i}\hbar T}{4m}\Big] \ .\end{aligned} \tag{3.22}$$

The remaining y-path integration gives for the free unrestricted motion the Green function

$$G(y'',y';E) = \frac{2m}{\hbar^2} I_{\sqrt{-2mE/\hbar^2+1/4}}(l\pi y_<) K_{\sqrt{-2mE/\hbar^2+1/4}}(l\pi y_>) \ , \tag{3.23}$$

therefore with $A_E(y) = I_{\sqrt{-2mE/\hbar^2+1/4}}(l\pi y)$, $B_E(y) = K_{\sqrt{-2mE/\hbar^2+1/4}}(l\pi y)$ for the Green's function in $y > 1$

$$G_{(y>1)}(y'',y';E) = \frac{2m}{\hbar^2}\Big\{A_E(y_>)B_E(y_<) - \frac{A_E(1)}{B_E(1)}B_E(y')B_E(y'')\Big\} \ . \tag{3.24}$$

This hyperbolic triangle billiard has been investigated by Graham et al. [14] in some detail, i.e., energy level statistics, spectral rigidity and the transition from a classical integrable system, i.e., the hyperbolic triangle billiard, to a classically chaotic system, i.e., motion in the modular domain. However, the determination of $P(\alpha)$ has not been done.

3.2.4 The hyperbolic ball.

The *hyperbolic sphere* is defined as a sphere in the Poincaré ball $B = \{(r,\vartheta,\varphi)|r < 1, \vartheta\in[0,\pi], \varphi\in[0,2\pi)\}$ endowed with the corresponding hyperbolic geometry $ds^2 = dr^2 + \sinh^2 r(d\vartheta^2 + \sin^2\vartheta d\varphi^2)$ [21]. Choosing $r = 1/\sqrt{2}$ yields $V = 4\pi$, and the quantization condition is given by the transcendental equation (assuming Dirichlet boundary conditions at $r = 1/\sqrt{2}$)

$$\mathcal{P}_{-1/2+\mathrm{i}p_n}^{-l-1/2}(3) = 0 \ , \qquad l = 0,1,\dots, \qquad n = 1,2\dots \ . \tag{3.25}$$

This quantization condition follows from the path integral representation in (pseudo-) spherical coordinates

$$\begin{aligned}&K(\tau'',\tau',\vartheta'',\vartheta',\varphi''\varphi';T)\\ &= \int\limits_{\tau(t')=\tau'}^{\tau(t'')=\tau''} \mathcal{D}_{(\tau<R)}\tau(t)\sinh^2\tau \int\limits_{\vartheta(t')=\vartheta'}^{\vartheta(t'')=\vartheta''} \mathcal{D}\vartheta(t)\sin\vartheta \int\limits_{\varphi(t')=\varphi'}^{\varphi(t'')=\varphi''} \mathcal{D}\varphi(t)\\ &\quad\times\exp\Big\{\frac{\mathrm{i}}{\hbar}\int_{t'}^{t''}\Big[\frac{m}{2}\big(\dot{\tau}^2 + \sinh^2\tau(\dot{\vartheta}^2+\sin^2\vartheta\dot{\varphi}^2)\big) - \frac{\hbar^2}{8m}\Big(4 - \frac{1}{\sinh^2\tau}\Big(1+\frac{1}{\sin^2\vartheta}\Big)\Big)\Big]dt\Big\}\\ &= (\sinh\tau'\sinh\tau'')^{-1}\sum_{l=0}^{\infty}\sum_{m=-l}^{l} Y_l^{m*}(\vartheta',\varphi')Y_l^m(\vartheta'',\varphi'')\\ &\quad\times\int\limits_{\tau(t')=\tau'}^{\tau(t'')=\tau''}\mathcal{D}_{(\tau<R)}\tau(t)\exp\Big\{\frac{\mathrm{i}}{\hbar}\int_{t'}^{t''}\Big[\frac{m}{2}\dot{\tau}^2 - \frac{\hbar^2}{2m}\frac{l(l+1)}{\sinh^2\tau}\Big]dt - \frac{\mathrm{i}\hbar T}{2m}\Big\} \ .\end{aligned} \tag{3.26}$$

Here the $Y_l^m(\vartheta,\varphi)$ are the spherical harmonics on the sphere. The quantization condition then follows from the corresponding Green function $G_{(\tau<R)}(E)$ by replacing in (3.16) $\nu\to l+1/2$. For $l>0$ the energy levels $E_n = p_n^2+1$ are $(2l+1)$-fold degenerate, and Weyl's law has the form

$$\bar{N}(E) \simeq \frac{6\sqrt{2}-\mathrm{arcosh}3}{3\pi}E^{3/2} - 2E + \frac{4\sqrt{2}-1}{3\pi}E^{1/2} - 1 \ . \tag{3.27}$$

4 Numerical Investigation.

4.1 Two-dimensional systems.

In figure 4.1 I have displayed for completeness the result for the rectangle billiard with $b = \pi/3$. We see that every feature is nicely confirmed, i.e., Weyl's law, the distribution of the normalized fluctuations, the number variance and the spectral rigidity, where $\Sigma_2(L)$ (average value) and $\Delta_3(L)$ saturate and $\Sigma_2(L) \simeq 2\Delta_3(L)$, as $L \to \infty$. For more details, c.f. [8, 13]. In table 4.1 I have also listed for comparison the effect of different values of b, i.e., $A = b$. For the investigation of the circle-billiard, which scales, see [27].

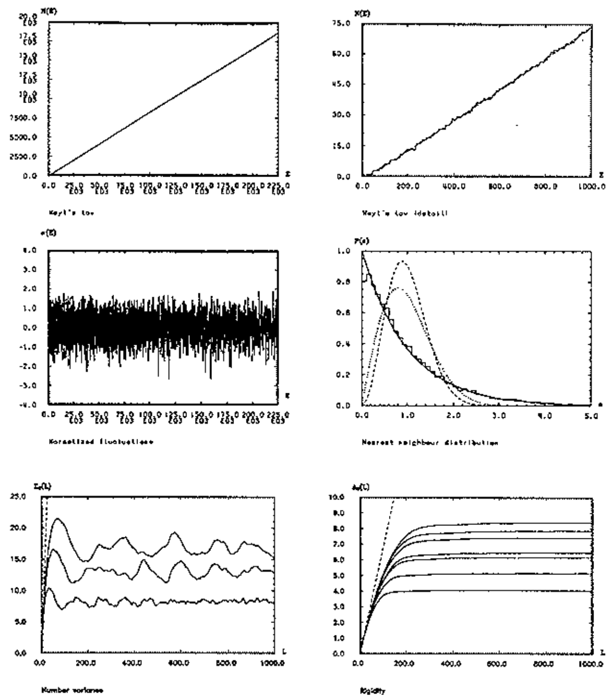

Figure 4.1: Analysis for the rectangle with $b = \pi/3$

In figure 4.2 I have displayed for the hyperbolic circle billiard the nice fitting of the spectral staircase (solid line) with Weyl's law (dashed line, c.f., the enlargement), the normalized fluctuations α_n, and the spectral rigidity $\Delta_3(L)$ for the number of energy levels of $\# = 1000, 2000, 2500, 3000, 4000, 5000$ and 10056, respectively, from which the number c_{Δ_∞} can be determined. Note that I have also incorporated the spectral rigidity for a Poissonian distribution with twofold degeneration (dashed line) $\Delta_3(L) = 2L/15$. All typical features of a classical integrable system are found. I omit the level-spacing statistics due to the degeneracy of the energy levels. Needless to say, $\Sigma_2(L) \simeq 2\Delta_3(L)$, as $L \to \infty$ (also omitted).

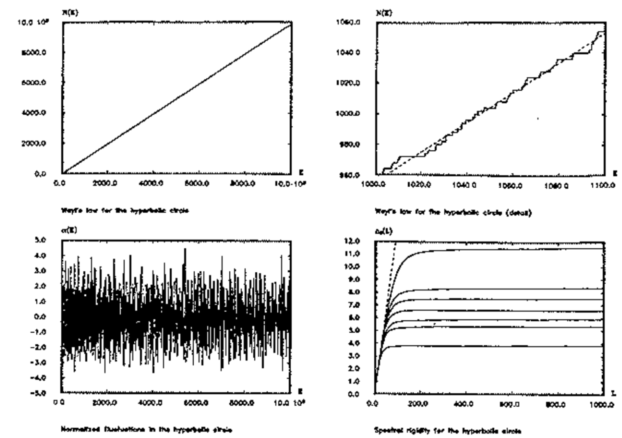

Figure 4.2: Analysis for the hyperbolic circle

Table 4.1: Comparison of the two-dimensional billiard systems

Billiard System	Area	# levels	E_{Max}	L_{Max}	c_{Δ_∞}	σ	κ
Euclidean Rectangle	4π	1 500	1 584	69	0.54	0.99	− 0.91
Euclidean Rectangle	2π	2 500	5 178	89	0.200	1.00	− 0.60
Euclidean Rectangle	π	6 100	24 810	138	0.094	1.01	− 0.77
Euclidean Rectangle	$\pi/2$	13 000	105 030	202	0.065	1.01	− 0.63
Euclidean Rectangle	$\pi/3$	19 000	229 890	244	0.0610	1.03	− 0.62
Euclidean Square	1	19 000	240 710	244	0.113	1.01	− 0.58
Euclidean Rectangle	1/20	1 000	271 770	56	1.14	0.97	− 0.83
Euclidean Circle	π	12 488	50 996	198	0.13	1.00	+ 0.20
Hyperbolic Rectangle	4π	943	1 011	56	0.102	1.02	− 0.75
Hyperbolic Rectangle	2π	466	1 011	39	0.093	1.02	− 1.03
Hyperbolic Rectangle	π	230	1 000	27	0.079	0.98	− 0.30
Hyperbolic Circle	4π	10 056	10 201	178	0.120	1.00	+ 0.40
Hyperbolic Circle	2π	750	1 566	49	0.14	0.99	+ 0.40
Hyperbolic Triangle	1/2	1 100	31 300	59	0.09	1.01	− 0.72

In figure 4.3a (top) I display the distribution of the normalized fluctuations for the the cases of the euclidean rectangle with area $A = 1, \pi, 4\pi$ and the euclidean circle with $R = 1$ (solid, dashed, dotted, dashed-dotted). The distributions have mean zero, standard deviation one (within the error margins), and are all skew, c.f., table 5.1; in particular the Euclidean square with $a = 4\pi$ stands out with an extremely fast decay for $\alpha \to \infty$, as is expected from the $e^{-c_2\alpha^4}$ behaviour, as $\alpha \to +\infty$.

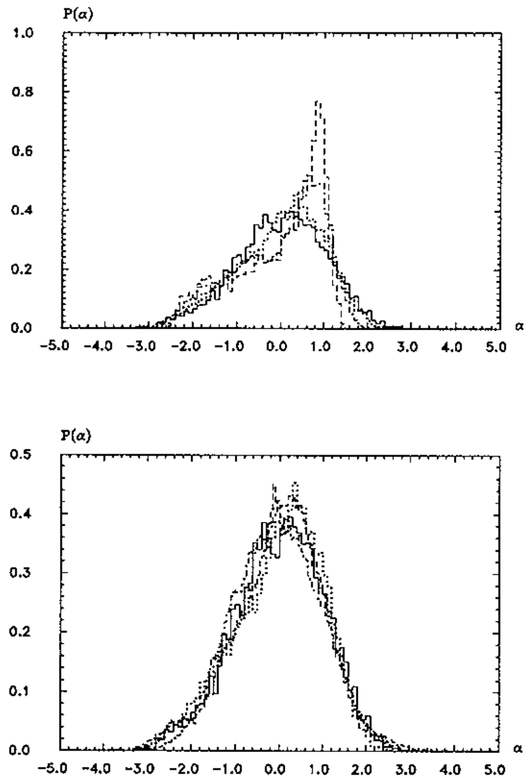

Figure 4.3: Distribution of deviations in the Euclidean plane (a,top) and in the hyperbolic plane (b,bottom).

In figure 4.3b (bottom) I display the distribution of the normalized fluctuations for the the cases of the hyperbolic rectangles with area $A = 4\pi, \pi$, the hyperbolic triangle with $A = 1/2$, and the hyperbolic circle with $A = 4\pi$ (dashed, solid and dotted, dashed-dotted line), respectively. Note that the distribution $P(\alpha_n)$ in hyperbolic geometry seems to be more regular, at least in the investigated systems.

The numerical results for the two-dimensional systems are summarized in table 4.1. # denotes the number of energy levels taken into account with E_{Max} the maximal energy. We observe nice confirmation of the semiclassical theory within an error margin of 3% in a wide energy range for billiard systems of different shape and geometry. The skewness κ can be considered as significant by means of a Kolmogorov-Smirnov test in comparison with a Gaussian distribution, e.g. [21]. Note that in all cases we observe a typical slow increase on the left side and a fast decay on the right side in the distributions in comparison to a Gaussian (which is omitted for graphical clarity), and the circle billiards have $\kappa > 0$.

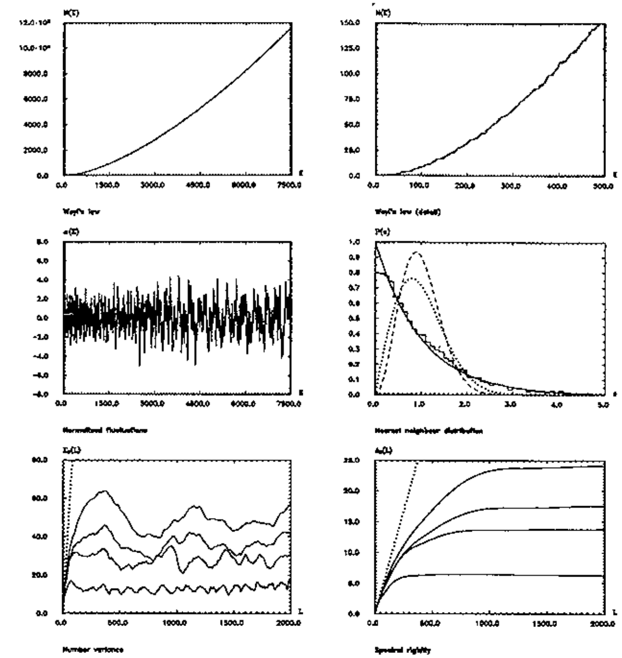

Figure 4.4: Analysis for the parallelepiped with $a = \pi/3$

4.2 Three-dimensional systems.

In figure 4.4 I have displayed the results for the $\pi/3$-parallelepiped with $a = \pi/3, b = a^2, c = a^3$. Due to the irrational relation of the lengths of the sides we have no energy level degeneracy, and the nearest neighbour statistics turns out to be Poissonian indeed in comparison to GOE (dotted) and GUE (dashed). Also, Weyl's law (and detail down to ground state) shows nice confirmation of the semiclassical theory. The fluctuations grow according to $\sqrt{E}$, which is confirmed by the shape of the normalized fluctuations. The number variance $\Sigma_2(L)$, which is displayed for $\# = 2500$, $\# = 5000\,\# = 10000$ and $\# = 11500$, and the spectral rigidity $\Delta_3(L)$, which is displayed for a maximum number of levels $\# = 2500$, $\# = 5000$, $\# = 10000$ and $\# = 11500$, respectively, from which c_{Δ_∞} can be determined, show saturation depending on L, where $\Sigma_2(L) \simeq 2\Delta_3(L)$, as $L \to \infty$, and with the correct L- and $L/15$-behaviour for $L \to 0$.

In figure 4.5 I have displayed the corresponding results for the hyperbolic ball-billiard, i.e., the comparison with Weyl's law, the normalized energy fluctuations, the number variance $\Sigma_2(L)$ (solid line), and the spectral rigidity (dotted line) in the entire range of the energy levels. Note the large jumps in the number of levels in comparison to Weyl's law due to the degeneracy of levels. I have displayed $\Sigma_2(L)$ for the maximum number of levels (dashed line), and $\Delta_3(L)$ for $\# = 5000$, $\# = 10000$, $\# = 20000$ and $\# = 27780$ (solid lines), respectively. Again, saturation for $\Sigma_2(L)$ and $\Delta_3(L)$ is observed.

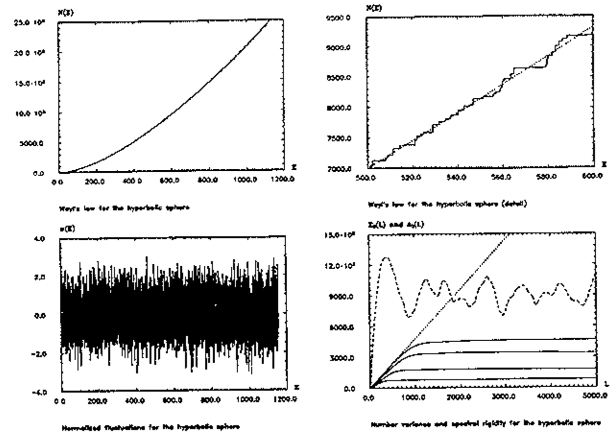

Figure 4.5: Analysis for the hyperbolic sphere

and $\Sigma_2(L) \simeq 2\Delta_3(L)$, as $L \to \infty$. The numerical results for the three-dimensional systems are summarized in table 4.2, including other parallelepipeds with $a = 1, \pi/2$ and $a = \pi$. Within an error margin of 8% all features of the semiclassical theory or confirmed. The large value for Δ_3 for the hyperbolic ball is easily explained by the high degeneracy of the levels which grows in average as $(2l+1)/2$, as can be easily checked (the dotted line denotes $\Delta_3(L) = 72L/15$ for a Poissonian distribution with a 72-fold degeneration because $l_{Max} = 72$ is the maximal angular momentum number within the considered energy range). The average value for c_{Δ_∞} turns out to be $c_{\Delta_\infty} = 0.17 \pm .01$.

Figure 4.6 finally shows the display of the deviations of the fluctuations of the various systems in three dimensions for the parallelepiped with $a = \pi/3$ (solid), $a = \pi$ (dotted), and the hyperbolic sphere (dashed). The distributions display a more regular (i.e. almost Gaussian behaviour), except that the distribution for the $a = \pi$ parallelepiped turns out to be more irregular, i.e. non-Gaussian as it should be. All distributions show the typical slow increase on the left side and the fast decay on the right side, as in two dimensions.

Table 4.2: Comparison of the three-dimensional billiard systems

Billiard System	Volume	# levels	E_{Max}	L_{Max}	c_{Δ_∞}	σ	κ
Euclidean Cube	1	13400	9021	205	0.014	1.08	− 0.5
Euclidean Epiped	$(\pi/3)^6$	11500	7443	190	0.0022	1.01	− 0.6
Euclidean Epiped	$(\pi/2)^6$	3000	1400	97	0.0040	0.93	− 0.8
Euclidean Epiped	π^6	500	122	40	0.045	1.02	− 1.2
Hyperbolic Sphere	4π	27 780	1156	285	0.17	0.97	+ 0.2

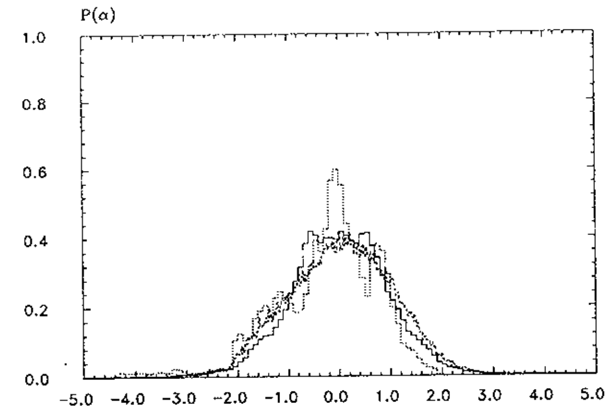

Figure 4.6: Distribution of deviations in three dimensions

5 Summary and Discussion

The presented results in this contribution show that the semiclassical theory of classically integrable billiard systems is in good agreement with the numerical results. This is not only the case for the flat billiard systems usually studied but also for billiard systems in spaces with (constant negative) curvature. The billiard system in the hyperbolic strip has been studied already, and I have included it in table 1 for completeness. The hyperbolic triangle billiard system has been studied in [14], but from a different point of view. The two new systems have been the hyperbolic circle- and the hyperbolic ball-billiard, the latter being a three-dimensional system. I have included an analysis for some flat parallelepipeds as well. All features predicted by the semi-classical theory have been found, i.e., fitting with Weyl's law, the growing of $\delta_n \propto E^{(d-1)/4}$ such that the normalized fluctuations α_n form a distribution $P(\alpha_n)$ with mean zero, deviation one, and (non-vanishing) skewness κ, and the typical features of the number variance and the spectral rigidity. It can also be observed that in the rectangular billiard with $b = \pi$ strong fluctuations in α_n appear which are due to bouncing ball modes according to Sieber et al. [32].

The problem of a analytical deviation of Δ_∞ and c_{Δ_∞} will be addressed elsewhere.

Of course, it is just a question of doing the numerical calculations and computer power to investigate more systems, may they be flat of hyperbolic. But I think the presented selection of systems shows already the typical features of classically integrable systems, and every more detailed study would only add "more statistics".

Acknowledgements

I would like to thank R.Graham and G.Vattay for sending me kindly some numerical data for analysis, and H.Primack, M.Sieber and F.Steiner for helpful information about billiard systems.

I would also like to thank the organizers J.Friedman, M.Gutzwiller and D.Hejhal of the IMA Workshop "Emerging applications of number theory", July 1996, Minneapolis, for the warm hospitality during my stay.

References

[1] R.Aurich, J.Bolte and F.Steiner: Universal Signatures of Quantum Chaos. *Phys.Rev.Lett.* **73** (1994) 1356–1359.

[2] R.Aurich and J.Marklof: Trace Formulæ for Three-Dimensional Hyperbolic Lattices and Application to Strongly Chaotic Systems. *Physica* **D 92** (1996) 101–129.

[3] R.Aurich, F.Scheffler and F.Steiner: On the Subtleties of Arithmetical Quantum Chaos. *Phys.Rev.* **E 51** (1995) 4173–4202.

[4] R.Aurich and F.Steiner: Energy-Level Statistics of the Hadamard-Gutzwiller Ensemble; *Physica* **D 43** (1990) 155–180.

[5] A.Bäcker, F.Steiner and P.Stifter: Spectral Statistics in the Quantized Cardioid Billiard. *Phys.Rev.* **E 52** (1995) 2463–2472.

[6] R.Balian and C.Bloch: Distribution of Eigenfrequencies for the Wave Equation in a Finite Domain. I. Three-Dimensional Problem with Smooth Boundary Surface. *Ann.Phys.(N.Y.)* **60** (1970) 401–447. Asymptotic Evaluation of the Green's Function for Large Quantum Numbers. *Ann.Phys.(N.Y.)* **63** (1971) 592–606. Distribution of Eigenfrequencies for the Wave Equation in a Finite Domain. II. Electromagnetic Field. Riemannian Spaces. *Ann.Phys.(N.Y.)* **64** (1971) 271–307. Distribution of Eigenfrequencies for the Wave Equation in a Finite Domain: II. Eigenfrequency Distributions. *Ann.Phys.(N.Y.)* **69** (1972) 76–160.

[7] H.P.Baltes and E.R.Hilf: Spectra of Finite Systems (*Bibliographisches Institut*, Mannheim, 1976).

[8] M.V.Berry: Semiclassical Theory of Spectral Rigidity. *Proc.Roy.Soc.(London)* **A 400** (1985) 229–251.

[9] M.V.Berry and M.Tabor: Level Clustering in the Regular Spectrum. *Proc.Roy.Soc.(London)* **A 356** (1977) 375–394.

[10] P.M.Bleher: On the Distribution of the Number of Lattice Points Inside a Family of Convex Ovals. *Duke Math.J.* **67** (1992) 461–481.
P.M.Bleher, Z.Cheng, F.J.Dyson and J.L.Lebowitz: Distribution of the Error Term for the Number of Lattice points Inside a Shifted Circle. *Commun.Math.Phys.* **154** (1993) 433–469.

[11] J.Bolte: Some Studies on Arithmetical Chaos in Classical and Quantum Mechanics. *Int.J.Mod.Phys.* **B 7** (1993) 4451–4553.

[12] T.A.Brody, J.Flores, J.B.French, P.A.Mello and S.S.M.Wong: Random-Matrix Physics: Spectrum and Strength Fluctuations. *Rev.Mod.Phys.* **53** (1981) 385–479.

[13] G.Casati, B.V.Chirikov and I.Guarneri: Energy-Level Statistics of Integrable Quantum Systems. *Phys.Rev.Lett.* **54** (1985) 1350–1353.

[14] A.Csordas, R.Graham, P.Szépfalusy and G.Vattay: Transition from Poissonian to Gaussian-Orthogonal-Ensemble Level Statistics in a Modified Artin's Billiard. *Phys.Rev.* **E 49** (1994) 325–332.
R.Graham, R.Hübner, P.Szépfalusy and G.Vattay: Level Statistics of a Noncompact Integrable Billiard. *Phys.Rev.* **A 44** (1991) 7002–7015.

[15] F.J.Dyson and M.L.Metha: Statistical Theory of the Energy Levels of Complex Systems. IV. *J.Math.Phys.* **4** (1963) 701–712.

[16] I.S.Gradshteyn and I.M.Ryzhik: Table of Integrals, Series, and Products (*Academic Press*, New York, 1980).

[17] C.Grosche: The Path Integral on the Poincaré Disc, the Poincaré Upper Half-Plane and on the Hyperbolic Strip. *Fortschr.Phys.* **38** (1990) 531–569.

[18] C.Grosche: Energy-Level Statistics of an Integrable Billiard System in a Rectangle in the Hyperbolic Plane. *J.Phys.A: Math.Gen.* **25** (1992) 4573–4594.

[19] C.Grosche: Path Integration via Summation of Perturbation Expansions and Application to Totally Reflecting Boundaries and Potential Steps. *Phys.Rev.Lett.* **71** (1993) 1–4.

[20] C.Grosche: δ-Function Perturbations and Boundary Problems by Path Integration. *Ann.Physik* **2** (1993) 557–589.

[21] C.Grosche: Path Integrals, Hyperbolic Spaces and Selberg Trace Formulæ (*World Scientific*, Singapore, 1996).

[22] M.C.Gutzwiller: Chaos in Classical and Quantum Mechanics (*Springer*, Berlin, 1990).

[23] R.U.Haq, A.Pandey and O.Bohigas: Fluctuation Properties of Nuclear Energy Levels: Do Theory and Experiment Agree? *Phys.Rev.Lett.* **48** (1982) 1086–1089.

[24] D.R.Heath-Brown: The Distribution and Moments of the Error Term in the Dirichlet Divisor Problem. *Acta Arithmetica* **40** (1992) 389–415.

[25] D.A.Hejhal: The Selberg Trace Formula for PSL(2, $\mathbb{R}$) I. *Lecture Notes in Mathematics* **548** (*Springer*, Berlin, 1976).

[26] H.Kleinert and I.Mustapic: Summing the Spectral Representations of Pöschl-Teller and Rosen-Morse Fixed-Energy Amplitudes. *J.Math.Phys.* **33** (1992) 643–662.

[27] I.Kim: Die Spurformeln für integrable und pseudointegrable Systeme. Diploma Thesis, Hamburg University, 1994. 113pp. (unpublished).

[28] D.V.Kosygin, A.A.Minasov and Ya.G.Sinai: Statistical Properties of the Spectra of Laplace-Beltrami Operators on Liouville Surfaces. *Russ.Math.Surveys* **48** (1993) 1–142.

[29] R.Schubert: The Trace Formula and the Distribution of Eigenvalues of Schrödinger Operators on Manifolds all of whose Geodesics are Closed. *DESY Report*, DESY 95-090, May 1995, 12pp.

[30] A.Selberg: Harmonic Analysis and Discontinuous Groups in Weakly Symmetric Riemannian Spaces with Application to Dirichlet Series. *J.Indian Math.Soc.* **20** (1956) 47–87.

[31] M.Sieber: The Hyperbola Billiard: A Model for the Semiclassical Quantization of Chaotic Systems. *DESY Report*, DESY 91-030, April 1991, Ph.D.Thesis (Hamburg University, 1991), 101pp.

[32] M.Sieber, U.Smilansky, S.C.Craegh and R.G.Littlejohn: Non-Generic Spectral Statistics in the Quantised Stadium Billiard. *J.Phys.A: Math.Gen.* **26** (1993) 6217–6230.

[33] M.Sieber and F.Steiner: Generalized Periodic-Orbit Sum Rules for Strongly Chaotic Systems. *Phys.Lett.* **A 144** (1990) 159–163.

[34] F.Steiner: Quantum Chaos. In "Schlaglichter der Forschung. Zum 75. Jahrestag der Universität Hamburg 1994", ed.: R.Ansorge (*Reimer*, Berlin, 1994), 543–564.